A probabilistic long-term framework for site-specific erosion analysis of wind turbine blades

A case study of 31 Dutch sites

Shankar Verma, Amrit; Jiang, Zhiyu; Ren, Zhengru; Caboni, Marco; Verhoef, Hans; van der Mijle-Meijer, Harald; Castro, Saullo G.P.; Teuwen, Julie J.E.

DOI
10.1002/we.2634

Publication date
2021

Document Version
Final published version

Published in
Wind Energy

Received: 28 August 2020 | Revised: 20 February 2021 | Accepted: 22 February 2021

DOI: 10.1002/we.2634

RESEARCH ARTICLE

WILEY

A probabilistic long-term framework for site-specific erosion analysis of wind turbine blades: A case study of 31 Dutch sites

Amrit Shankar Verma[1,2] | Zhiyu Jiang[3] | Zhengru Ren[4] | Marco Caboni[5] | Hans Verhoef[5] | Harald van der Mijle-Meijer[5] | Saullo G.P. Castro[1] | Julie J.E. Teuwen[1]

[1]Faculty of Aerospace Engineering, Delft University of Technology (TU Delft), Delft, Netherlands

[2]Department of Ships and Ocean Structures, SINTEF Ocean AS, Trondheim, Norway

[3]Department of Engineering Sciences, University of Agder, Grimstad, Norway

[4]Department of Marine Technology, Norwegian University of Science and Technology (NTNU), Trondheim, Norway

[5]TNO Energy Transition, Petten, The Netherlands

Correspondence
Amrit Shankar Verma, Faculty of Aerospace Engineering, Delft University of Technology (TU Delft), Delft 2629 HS, The Netherlands.
Email: a.s.verma@tudelft.nl

Funding information
Rijksdienst voor Ondernemend Nederland, Grant/Award Number: TEHE118013 (Windcore)

Abstract

Rain-induced leading-edge erosion (LEE) of wind turbine blades (WTBs) is associated with high repair and maintenance costs. The effects of LEE can be triggered in less than 1 to 2 years for some wind turbine sites, whereas it may take several years for others. In addition, the growth of erosion may also differ for different blades and turbines operating at the same site. Hence, LEE is a site- and turbine-specific problem. In this paper, we propose a probabilistic long-term framework for assessing site-specific lifetime of a WTB coating system. Case studies are presented for 1.5 and 10 MW wind turbines, where geographic bubble charts for the leading-edge lifetime and number of repairs expected over the blade's service life are established for 31 sites in the Netherlands. The proposed framework efficiently captures the effects of spatial and orographic features of the sites and wind turbine specifications on LEE calculations. For instance, the erosion is highest at the coastal sites and for sites located at higher altitudes. In addition, erosion is faster for turbines associated with higher tip speeds, and the effects are critical for such sites where the exceedance probability for rated wind conditions are high. The study will aid in the development of efficient operation and maintenance strategies for wind farms.

KEYWORDS
coatings, leading-edge erosion, operation and maintenance, wind energy, wind turbine blades

1 | INTRODUCTION

In order to account for the rising carbon levels in the atmosphere, there is a substantial increase in the demand of renewable sources of energy. Among all the sources, wind energy owing to its abundant resource availability and decades-long technical maturity, is one of the fastest growing renewable sectors.[1] Europe has been the front runner in the wind energy sector, and a recent report suggests that wind energy could become the largest power source by 2050.[2] In order to achieve this, a significant increase is expected in the number of turbines being deployed, both in onshore and offshore sectors, along with improved technological advances. One of the methods to improve the efficiency and energy production from the wind turbines is to increase the blade size that advances the total rotor swept area and improves the overall power capacity of the turbine.[3-5] However, increased blade length also poses major design constraints to the blade designer and maintenance constraints to the wind farm owners. Wind turbine blades (WTBs) of lengths 70–75 m can be associated with high tip speed, in the range of 75–90 m/s.[6,7] Due to recurring

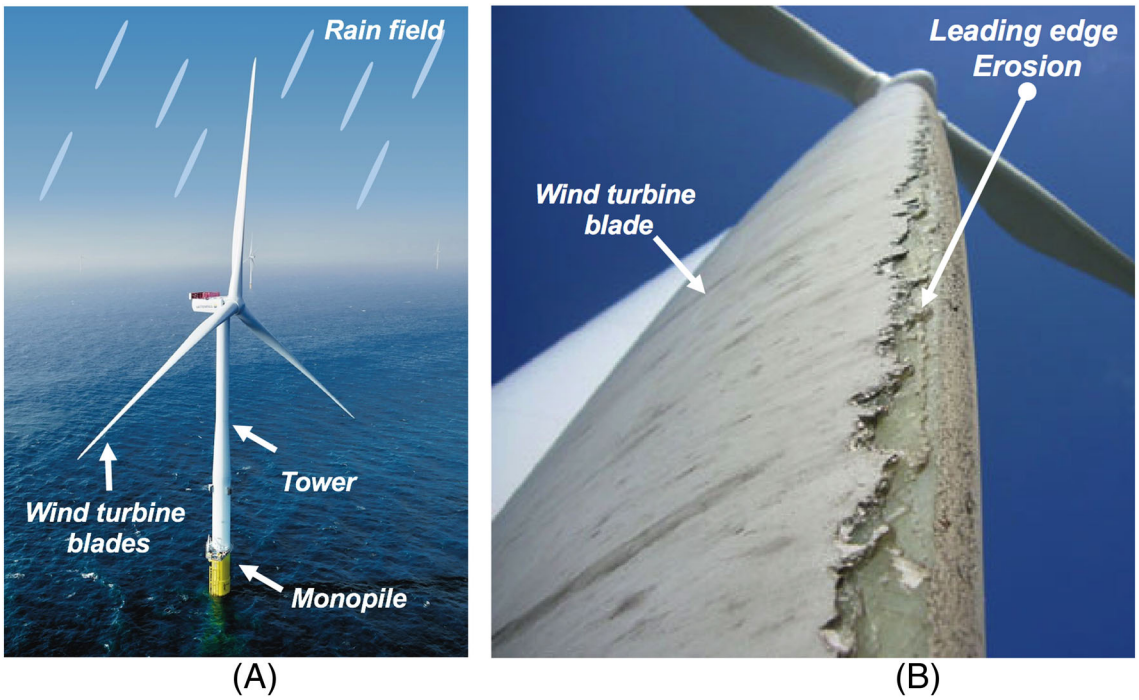

FIGURE 1 (A) Wind turbine exposed to rain field.[17] (B) Example of LEE of WTB[18]

contact with rain during their service life (Figure 1A), WTBs can suffer material degradation at their leading edges (Figure 1B). This material degradation leading to the roughening of leading-edge surface and subsequent material loss is designated as rain-induced leading-edge erosion (LEE) of WTBs.[8]

The roughening of the surface due to LEE causes a reduction in the aerodynamic performance of the WTBs as well as the power output of the turbine.[9] As a result, regular inspection and repair activities are required to be carried out to rectify the damaged profile of the leading edge, which adds significant costs to the overall energy produced.[10,11] It has been reported that the effects of LEE can trigger in less than 1 to 2 years for some of the wind turbine sites, while it may take several years for other sites.[12,13] As a result, different wind turbine sites display a very distinct erosion lifetime for the same blade coating system and need site-specific inspection and repair requirements.[12] The site-specific variation in the LEE performance of coatings comes from the fact that wind and rain conditions govern the erosion of WTBs and their statistical parameters exhibit a stochastic nature.[14,15] In other words, the probability of occurrence of wind and rain conditions and their associated statistical parameters vary from site to site[16] and this makes LEE a site-specific problem. Consequently, tools and methods are required that enable site-specific estimation of the expected lifetime of the blade coating system and treat rain and wind parameters as stochastic.

In the current study, a probabilistic long-term framework is proposed for assessing the site-specific expected lifetime of a WTB coating system. To the best of the authors' knowledge no such framework exists which has been applied to LEE of WTBs and thus reflects the novelty of this work. Also, one of the main goals of this paper is to propose this framework as an efficient way to perform analysis during the pre-design phase to select a suitable coating system for a given wind turbine site and perform LEE calculations. Further, case studies are presented for a 1.5 and 10 MW turbine where *geographic bubble chart*[1] for the leading-edge lifetime and number of repairs expected during the blade's service life are established for 31 sites in the Netherlands. The remainder of the paper proceeds as follows: Section 2 presents a brief literature review on the state of the art LEE models. Section 3 presents the proposed framework, methodology as well as details on the case study. Section 4 presents and discusses the results. Section 5concludes the paper and finally section 6 presents the limitations and recommendation for future work.

2 | LITERATURE REVIEW: LEE MODELS

In the literature, there have been several efforts in developing erosion models to predict the leading-edge performance of the blade coating system against rain-induced erosion. These models in general require different input parameters since LEE of WTBs is a result of simultaneous

[1]Geographic bubble chart is a technique of presenting the data as filled, coloured circles, referred to as bubbles, at different position on a geographical map marked with longitude and latitude. The bubble's size and colour can be used to represent magnitude and intensity of data values at these locations.

interplay of several factors such as rain and wind parameters interacting with the blade coating system during operations. Figure 2 presents a general framework of a typical LEE model with different input and output parameters. The input parameters include (1) *rainfall statistical model* consisting of stochastic inputs such as rainfall intensity, rainfall duration as well as the rain droplet size that determine the rain loading on the blade during its service life, (2) *wind turbine model* that includes defining the mean wind speed at the hub height which is a stochastic input as well as defining the turbine's rotations per minute (RPM) schedule that determines the tip speed of the blade, (3) *an impingement model* that determines the number of droplets that will actually hit the WTB during rotation, and (4) *coating material model* that includes fatigue and mechanical properties of the coating and characterises the erosion resistance of the coating material. These parameters are then fed into a LEE model and different output parameters are calculated such as (1) incubation period that refers to the time period before any mass loss is seen in the coating and is referred to as 'expected leading-edge (LE) lifetime of blade coating system' in this paper,[19] (2) rate of mass loss that represents a stage where the mass is lost at a steady rate, and (3) total time to failure which describes complete removal of coating materials. In addition to these results, other parameters are also of interest such as the analysis of impact stresses,[14] fatigue cracks,[4,20] and surface roughness growth[21] due to recurring droplet impact onto the coating.

The above mentioned LEE models can either be a phenomenological-based analytical model or a pure numerical computational model.[4] The computational models range from coupled fluid structure interaction models such as the Smooth Particle Hydrodynamic (SPH) methods[8,22] and the Coupled Eulerian Lagrangian methods (CEL),[10,23] to a more conventional decoupled computational fluid dynamics (CFD)-finite element method (FEM) calculations.[24] Most studies using such models are deterministic in nature and analyse single rain droplet impact response on the coated panels to investigate the underlying erosion mechanism process, under averaged environmental and operation conditions. While these models capture the realistic droplet impingement process to a very high degree of precision, such models are still too complex and computationally demanding, and may not be an efficient choice at the preliminary design stage. In addition, it is not straightforward to extrapolate the results from the single droplet to include the effects of multiple rain droplets hitting the blade in a random manner.[6] Nevertheless, attempts have been made to propose frameworks where different parameters shown in Figure 2 are included to calculate erosion damage of a coating. A computational framework was presented in Amirzadeh et al.[24,25] where stochastic rain texture model was coupled with the results from CFD-FEM code to evaluate the expected fatigue life of the blade coating. Recently another computational framework[4] consisting of multi-axial critical plane fatigue model of coating degradation was proposed based on the assumption that no two successive droplets overlap with each other while impacting the blade during precipitation. Although these computational frameworks are promising and include randomness in the number and size of drops hitting the blade surface area, the requirement of a framework that treats rain and wind parameters as stochastic and aids site-specific analysis of LEE has still not been achieved.

Compared to the computational models, analytical-based LEE models present a more simplified analysis of LEE of WTBs. There are many analytical-based models utilised in the literature such as Springer's surface fatigue model for homogeneous,[26] coated[27] and fibre-reinforced material,[28,29] DTU's Kinetic energy model,[30] Siemens erosion model,[19] micromechanical model for Polyurethane coatings[31] and TNO's fatigue model.[32,33] Though the above models have several assumptions inherent in their formulations, they still represent a sound physical representation of droplet impingement process onto the coating system. These models give first order estimates of parameters such as water hammer pressure, incubation time as well as total time to failure to name a few. In addition, they efficiently couple different input models shown in Figure 2 along

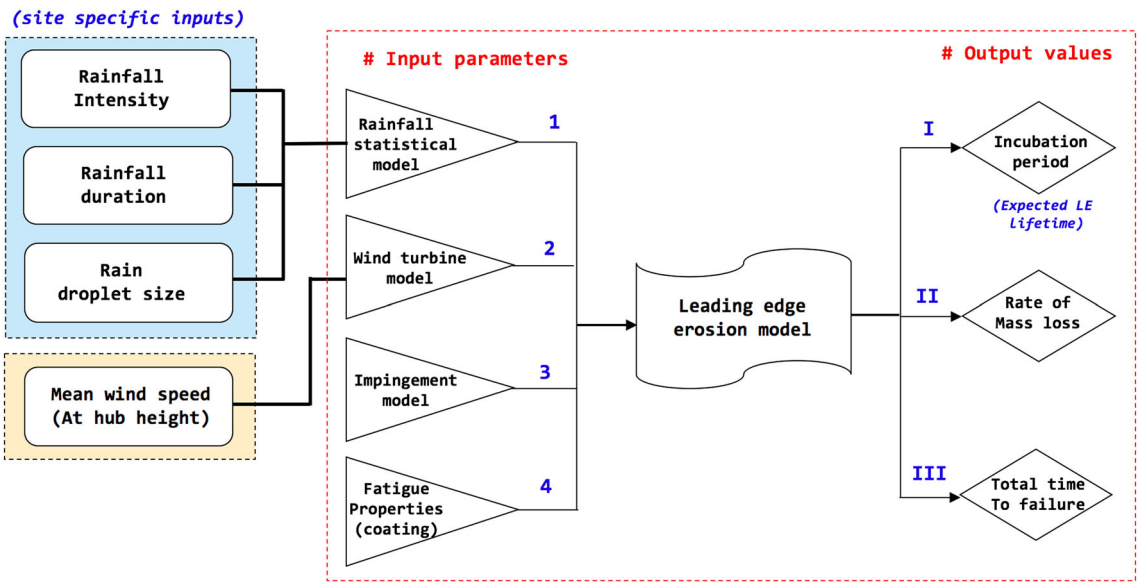

FIGURE 2 General architecture of LEE model with input and output parameters

with the total number of drops contained in a rainfall to estimate the expected lifetime of a blade coating system. However, one of the main shortcomings of these models is that the estimates from such an analysis represent the accelerated erosion of coatings based on deterministic load cases and it is not straightforward to include all possible rain and wind loading conditions for site-specific erosion analysis. Generally, representative load cases such as the median droplet sizes based on a few popular droplet size distributions (DSDs) for extreme rain cases are considered, based on which the erosion damage rate of a WTB is calculated.

In view of these shortcomings, there have been efforts to extend the scope of the above discussed analytical erosion models and perform site-specific analysis of LEE of WTBs. Hasager et. al[12] performed analysis on a 3.2 MW WTB in the Danish Seas using the kinetic energy based LEE model and considered five coastal and three inland sites. The results of the studies showed that the erosion of WTB coating system is approximately 4 times higher for the coastal sites compared to the inland sites because of higher occurrence of heavy rain at large wind speeds. The study provided a comprehensive discussion on erosion dependence on statistical characteristics of rain and wind conditions for a given site, although the study lacked a pure probabilistic framework. It was also hypothesised that extreme rain events are significantly important during erosion calculations, however, all rain events contributed to the fatigue of the blade surface. Another attempt has been made by the authors of the present paper to propose a probabilistic rainfall model in Verma et al.[14] to establish rain and wind characteristics in terms of different probabilistic distributions. Those analyses were performed on a 5 MW wind turbine using the Springer's surface fatigue model[26] where the case studies include one coastal and one inland Dutch site. It was found that the erosion lifetime for a WTB is 3 to 4 times less for turbines operating at coastal sites compared to the inland sites based on the hypothesis that the observed erosion was a result of recurring exposure to all possible rain and wind conditions. The current paper proposes a probabilistic long-term framework as an extension of this previous study in Verma et al.,[14] where the probabilistic rainfall model was proposed. In the framework, the probabilistic rainfall model is combined with other input parameters such as wind statistics model, wind turbine model, and coating material model and the leading-edge lifetime of a WTB coating system is evaluated for different sites.

3 | METHODOLOGY AND CASE STUDY

Figure 3 presents the flowchart describing the analysis procedure for the long-term probabilistic framework proposed in this study. The flowchart describes how different input models—probabilistic rainfall model, wind statistics model, wind turbine model, and coating material model (shown in varying background colours) are connected to the analytical surface fatigue model to calculate the site-specific leading-edge lifetime of WTB coating system. The main outcome of the proposed model is to obtain a geographic bubble chart of leading-edge lifetime for all the chosen sites as well as number of repairs expected over a turbine's lifetime. A brief summary of the description of the sites, models that make up the long-term framework as well as the details of the case study is described below:

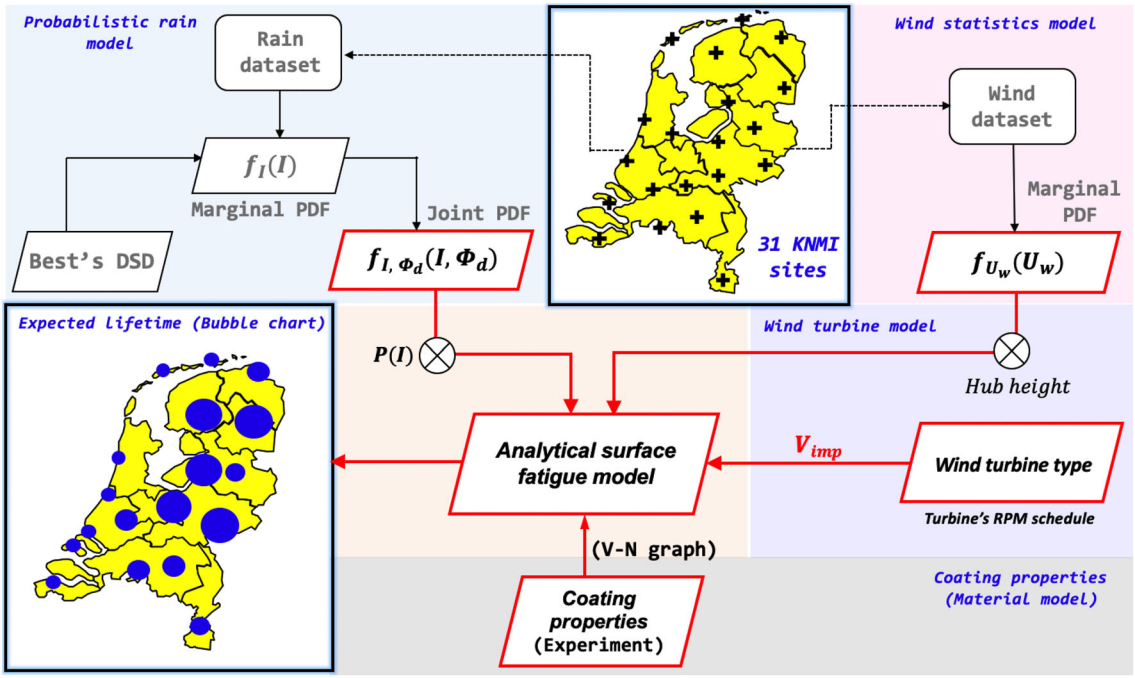

FIGURE 3 General analysis procedure and long-term probabilistic framework

TABLE 1 Details of different Dutch sites considered in the analysis

Station number	Site name	Longitude (east) (degrees)	Latitude (north) (degrees)	Altitude (m)
210	Valkenburg	4.430	52.171	−0.200
235	De Kooy	4.781	52.928	1.200
240	Schiphol	4.790	52.318	−3.300
249	Berkhout	4.979	52.644	−2.400
251	Hoorn (Terschelling)	5.346	53.392	0.700
260	De Bilt	5.180	52.100	1.900
267	Stavoren	5.384	52.898	−1.300
269	Lelystad	5.520	52.458	−3.700
270	Leeuwarden	5.752	53.224	1.200
273	Marknesse	5.888	52.703	−3.300
275	Deelen	5.873	52.056	48.200
277	Lauwersoog	6.200	53.413	2.900
278	Heino	6.259	52.435	3.600
279	Hoogeveen	6.574	52.750	15.800
280	Eelde	6.585	53.125	5.200
283	Hupsel	6.657	52.069	29.100
286	Nieuw Beerta	7.150	53.196	−0.200
290	Twenthe	6.891	52.274	34.800
310	Vlissingen	3.596	51.442	8.000
319	Westdorpe	3.861	51.226	1.700
323	Wilhelminadorp	3.884	51.527	1.400
330	Hoek van Holland	4.122	51.992	11.900
344	Rotterdam	4.447	51.962	−4.300
348	Cabauw	4.926	51.970	−0.700
350	Gilze-Rijen	4.936	51.566	14.900
356	Herwijnen	5.146	51.859	0.700
370	Eindhoven	5.377	51.451	22.600
375	Volkel	5.707	51.659	22.000
377	Ell	5.763	51.198	30.000
380	Maastricht	5.762	50.906	114.300
391	Arcen	6.197	51.498	19.500

3.1 | Description of the sites

In this study, 31 Dutch sites corresponding to the KNMI[2] weather stations in the Netherlands (see Table 1 and Figure 4A) have been considered. These stations are chosen in such a way that the entire Netherlands is covered in this analysis. The precipitation and wind data for each station are obtained from the KNMI database for the last 25 years. The precipitation data is measured using rain gauge and consists of information such as the total amount of rainfall (mm) at a given site and the data is available for each hour. Further, the data for the mean wind speed is available at 10 m reference height. Choosing these many sites is advantageous as this will provide a verification study for the proposed framework. For instance, several stations corresponding to different inland and coastal sites are considered and thus this is expected to give a varying erosion lifetime. Also, these stations considered in the study are associated with varying altitudes above the sea level (see Table 1 and Figure 4B) and thus the orographic effects on LEE calculation can be captured using the proposed framework. It is to be noted that most of the sites in the Netherlands have altitudes below or just above the sea level (Table 1). However, some of the sites such as Maastricht (station no. 380) and Deelen (station no. 275) have an altitude of 114.8 and 48.2 m, respectively.

[2]Koninklijk Nederlands Meterorologisch Instituut (KNMI): KNMI is the Dutch weather forecasting service that performs weather forecasting, climate monitoring and tasks related to seismology.

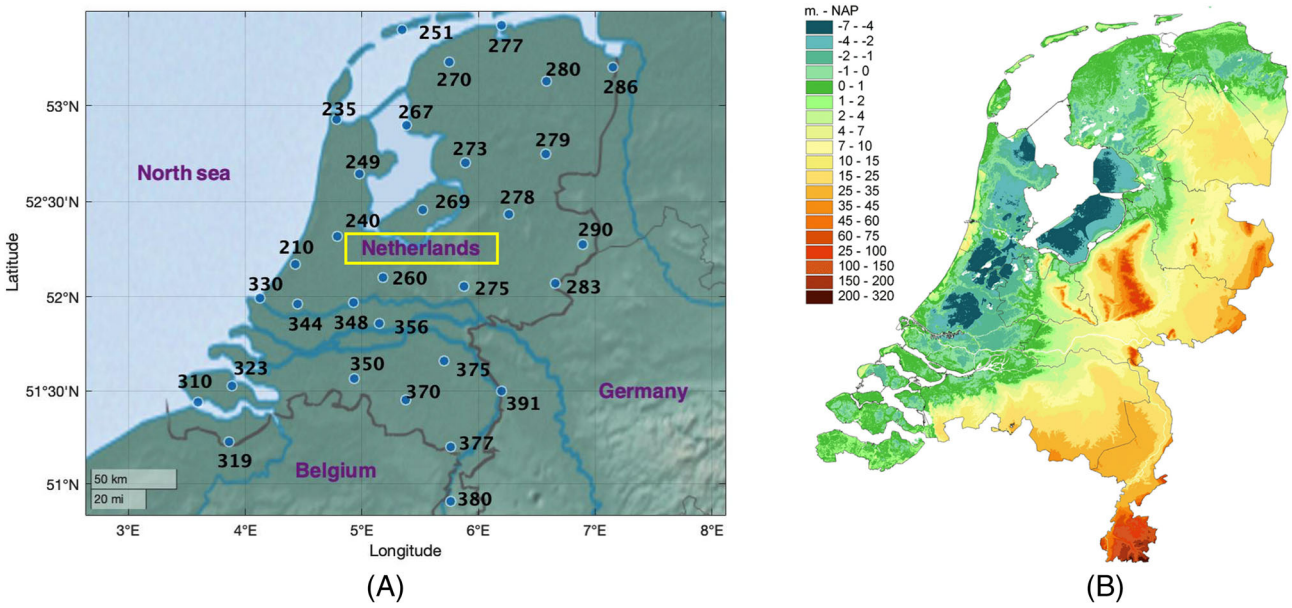

FIGURE 4 (A) Different stations considered in the analysis. (B) Topography of the Netherlands[35]

3.2 | Probabilistic rainfall model

The first input parameter for the proposed framework in this study is the probabilistic rainfall model. This model has been discussed elsewhere by the Verma et al.[14] and is summarised here briefly for completeness of discussion. The probabilistic rainfall model describes the rain statistical parameters through the joint probabilistic distributions of rain droplet size (ϕ_d) and rainfall intensity (I) along with a correction factor ($P(I)$) that describe the percentage of time rain of a given intensity falls at a given site. Given that the droplet size and rain intensity are statistically dependent random variables, the joint probability distribution function of ϕ_d and I is given by the relation

$$f_{I,\phi_d}(I,\phi_d) = f_I(I) \cdot f_{\phi_d|I}(\phi_d|I) \tag{1}$$

where $f_I(I)$ is the marginal probability distribution of rain intensity, and $f_{\phi_d|I}(\phi_d|I)$ is the droplet size distribution (DSD) that describes the distribution of droplet size for a given rainfall intensity. Note that both the distributions are site-specific; however, in this study, only the rainfall intensity is varied for all the 31 Dutch sites. Although the DSD can be obtained using the disdrometer, it was not available for the considered Dutch sites at the time when this study was performed. Instead, one of the most popular Best's DSD[34] is considered for all chosen sites which is given by

$$F_{\phi_d|I}(\phi_d|I) = 1 - exp\left[-\left(\frac{\phi_d}{1.3I^{0.232}}\right)^{2.25}\right] \tag{2}$$

Note that this assumption may underestimate the lifetime calculated for the wind turbines installed at the coastal sites as shown in Verma et al.[14] and Shankar Verma et al.,[36] but it shouldn't affect the main findings and conclusions of the paper. Figure 5 presents the probability density function (PDF) of droplet size for different rain intensities (I = 0.1, 1, 10, 25 mm/h) using Best's DSD. It can be seen from the figure that the contribution of bigger droplet sizes in a given rain increases with increasing rainfall intensity. For obtaining the most appropriate distribution fit for the rainfall intensity, lognormal and gamma distributions are compared[37,38] for all the sites and their distribution parameters are obtained using maximum likelihood estimation (MLE) method. A goodness of fit test is also performed using the chi-square (χ^2) method. The probability density function (PDF) of the lognormal distribution is given by

$$f(x) = \frac{1}{\sqrt{2\pi}\sigma_x} e^{-(\ln(x)-\mu_x)^2/2\sigma_x^2} \;;\; x > 0, \text{ and } \sigma_x > 0 \tag{3}$$

where μ_x and σ_x are parameters of the distribution and are defined as mean and standard deviation of logarithmic data, respectively. On the other hand, gamma distribution is given by

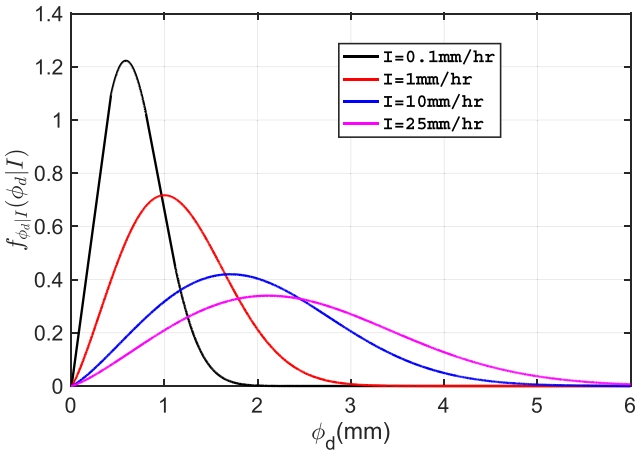

FIGURE 5 Probability density function of droplet size based on Best's DSD

$$f(x) = \frac{x^{\alpha-1}e^{-x/\beta}}{\beta^{\alpha}\Gamma(\alpha)}\ ;\ x > 0,\ \text{and}\ \alpha > 0,\ \beta > 0 \tag{4}$$

where α and β are shape and scale parameters, respectively. $\Gamma(\alpha)$ is called as the gamma function and is given by

$$\Gamma(\alpha) = \int_0^{\infty} x^{\alpha-1}e^{-x}dx \tag{5}$$

χ^2 goodness of fit testing is performed by comparing χ^2 obtained from the equation below using the rain data and comparing with χ^2_{cric}. The χ^2 is given by the relation

$$\chi^2 = \sum_{k=1}^{n} \frac{(O_k - E_k)^2}{E_k} \tag{6}$$

and χ^2_{cric} value is obtained from the standard χ^2 curve that depends on the significance level which is assumed 5% (95% confidence level) and degree of freedom is determined by the expression: $n - 1 - m$. Here n is the number of bins the data is divided into and m is the number of distribution parameters which is 2 for both lognormal and gamma. If χ^2 is found less than χ^2_{cric}, then the distributions supported by the null hypothesis statement cannot be rejected at the chosen significance level.

3.3 | Wind statistics model

The wind statistics model is described by determining the best distribution fit for the mean wind speed at the hub height of the turbine. Given that the data for all the stations are available at 10 m reference height, mean wind speed at the desired hub height using the power law is given by

$$U_w(z) = U_w(z_r) \cdot \left(\frac{z}{z_r}\right)^{\bar{\alpha}} \tag{7}$$

where $U_w(z)$ is the mean wind speed at the hub height, $U_w(z_r)$ is the mean wind speed at the reference height of 10 m, and α is the power law exponent taken as 0.14 in this study based on the IEC guidelines.[39] The two-parameter Weibull distribution is considered as the best distribution fit for wind statistics, which is acceptable for describing the mean wind speed in the literature.[40] Nevertheless, a preliminary check is also made by plotting the wind speed data on the Weibull and lognormal probability paper. The PDF of the two-parameter Weibull distribution is given by

$$f_{U_w}(u) = \frac{\alpha_u}{\beta_u}\left(\frac{u}{\beta_u}\right)^{\alpha_u - 1} \cdot exp\left[-\left(\frac{u}{\beta_u}\right)\right]^{\alpha_u} \tag{8}$$

where α_u and β_u are shape and scale parameter which are obtained by using maximum likelihood estimation (MLE) method.

3.4 | Wind turbine model

The wind turbine model is represented by the turbine's rotations per minute (RPM) schedule which determines the rotor speed for a given mean wind speed. This is a necessary curve for the model that will govern the impact velocity between rotor blade and rain droplets during the operations. In addition, other specifics of the turbine such as length of WTBs and hub height are essential to describe the kinematics of rain droplet impact during operation.

3.5 | Analytical LEE model and coating properties

In order to understand the long-term framework proposed in this study, it is essential to understand the concept of short-term erosion damage and long-term erosion damage. These terms are well known in the marine community to calculate the fatigue damage of offshore structures[41,42] and operability analysis of marine operations.[43-46] Here, both the terms and their associated equations applied to LEE of WTBs are described.

3.5.1 | Short-term erosion damage

The erosion damage calculated using the analytical LEE models such as the Springer's surface fatigue model[29] can be referred to as the short-term erosion damage. Here, the erosion analysis of a given coating is performed without considering the probability of occurrence of rain and wind conditions and represent accelerated erosion. It is assumed that the coating is continuously exposed to the deterministic rain loading cases with no dry periods[3] considered, based on which the incubation period is calculated. In this study, an analytical surface fatigue model from Springer[29] is used to describe the short-term erosion damage which is given by

$$\dot{D}_i^{ST}(I,\phi_d,U_w) = \frac{\bar{q}\cdot V_{imp}\cdot\beta_d}{\frac{8.9}{\phi_d^2}\left(\frac{S}{p_{wh}}\right)^{5.7}} \tag{9}$$

where $\dot{D}_i^{ST}(I,\phi_d,U_w)$ is the short-term erosion damage rate of a coating for a given rain load described by deterministic combinations of I, ϕ_d and U_w. V_{imp} in the above equation is defined as the magnitude of the impact velocity between individual raindrop and the blade that is approximately given by

$$V_{imp} = V_{blade} + V_{tg} \tag{10}$$

where V_{blade} is defined as the blade tip speed and depends upon the operational mean wind speed (U_w). V_{tg} is defined as the perpendicular terminal speed of an individual rain droplet and is dependent upon the rain droplet size (ϕ_d) defined in mm, V_{tg} (in m/s) is given by the relation[47]

$$V_{tg} = 9.65 - 10.3e^{-0.6\phi_d} \tag{11}$$

$\bar{q}$ is the number of rain droplets per unit volume of rainfall which is given by

$$\bar{q} = 530.5\frac{I}{V_{tg}\phi_d^3} \tag{12}$$

where I is the intensity defined in mm/h. β_d is the fraction of droplet that will hit the blade during rotation (impingement efficiency) and is given by the relation[48]

$$\beta_d = 1 - e^{-15\phi_d} \tag{13}$$

p_{wh} is the water hammer pressure defined by

[3]Dry period is considered as the period of time when there is no occurrence of rain at the wind turbine site. In general, rotation of blade during the dry period is not expected to contribute towards rain-induced erosion of WTBs.

$$p_{wh} = \frac{\rho_w c_w V_{imp}}{1 + \frac{\rho_w c_w}{\rho_s c_s}} \tag{14}$$

where ρ_w and c_w are density of water (1000 kg/m^3) and speed of sound in water (1480 m/s), ρ_s and c_s are density of coating and speed of sound in the coating material, respectively. S is the erosive strength of coating material defined by

$$S = \frac{4\sigma_u(m-1)}{1-2\nu} \tag{15}$$

where σ_u, m and ν are the ultimate tensile strength, Wöhler slope and Poisson's ratio of the coating material, respectively. Note that a Polyurethane (PU) based coating material is used for the analysis in this study. The Wöhler slope (m) for the coating is an essential material parameter and is obtained by performing experiments in this work using the droplet impingement test and is discussed briefly below.

Experiment: Determination of Wöhler slope (m)

Droplet impingement test on the PU based coating system is carried out using Ducom droplet erosion tester[49] (Figure 6A–C). The Ducom droplet erosion tester can simulate the accelerated erosion by repetitive droplet impingement onto the coating, and different test parameters, such as impact velocity, droplet size, impact frequency and droplet impact angle, can be varied. The instrument produces the high velocity water droplets by cutting a high pressure water jet flowing through a nozzle by obstructing it with a rotating disc. In this study, the accelerated erosion is performed for five different impact velocities (V_d) ranging between 120 and 200 m/s, and the number of impacts (N) until the incubation period is recorded. The incubation period is considered as the point of instant when the evidence of first surface damage is observed. In this way, a '$V_d - N$' graph is obtained for the coating system as shown in Figure 7A,B. Here, the results represent mean of the incubation time measured using six different coated samples to include the effects of variability. All the tests are performed for normal impingement (90^o impact angle), using a rotating disc that produces 2 mm droplet diameter. The method presented by Slot et al.[33] and DNVGL.[50] is used to estimate the Wöhler slope

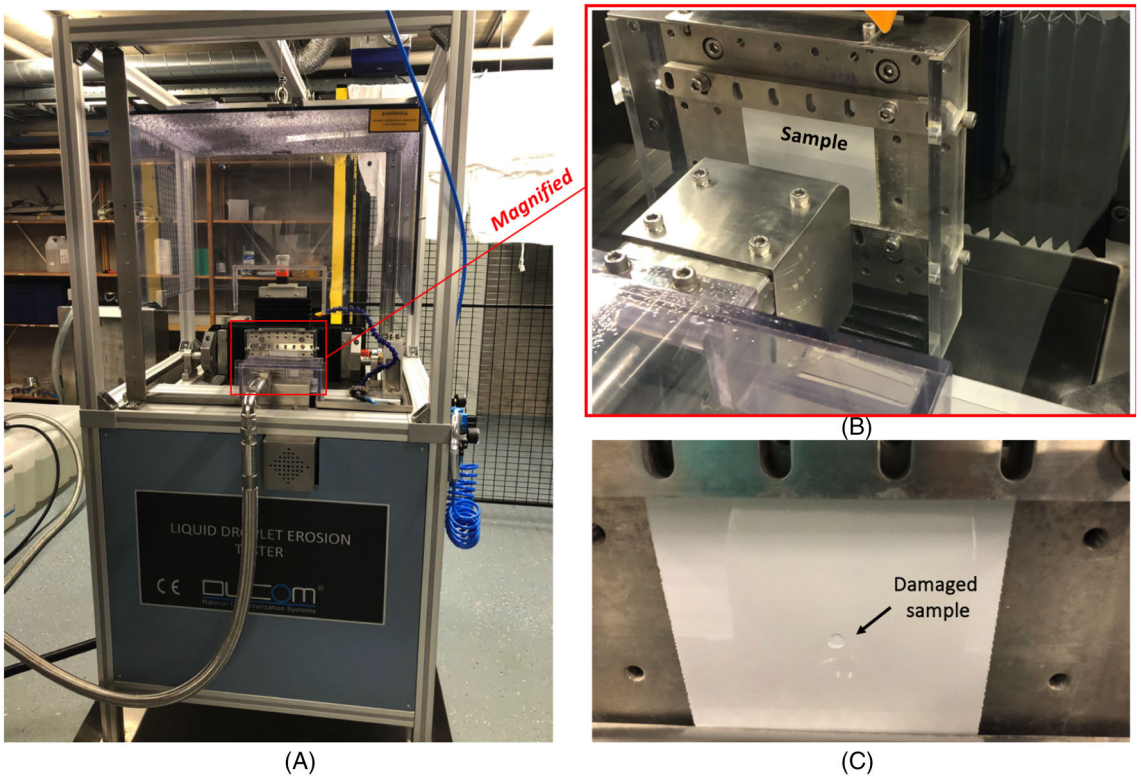

FIGURE 6 (A) Experimental setup. (B) PU sample (shown in white). (C) An example of droplet damage onto the coating

(m) of the coating from the test results. First, the velocity of impact (V_d) and the recorded number of impacts (N) until the incubation period is fitted through a power law which is given by[50]

$$N = k \cdot V_d^m \tag{16}$$

Here, k and m are obtained as (9.9e40) and (−16.92), respectively (Figure 7A). Further, the above relation is then transformed such that the below equation gives the Wöhler slope (m) for the coating material. This equation is given by

$$log(N) = log(k) + m \cdot log(V_d) \tag{17}$$

For the considered coating, m is obtained as 16.92 (Figure 7B). Other coating properties are obtained from the manufacturer's datasheet as well as other literature sources that are summarised in Table 2.

Long-term erosion damage

Unlike the short-term erosion damage discussed above, the long-term erosion damage considers erosion analysis by including the probability of occurrence of rain and wind conditions. It considers the damage on a structure as a result of continuous long-term exposure to environmental factors, such as exposure of blade to rain and wind condition throughout the service life. The long-term erosion damage rate of coating is given by the weighted sum of short-term erosion damage rate contributed from all possible rain and wind conditions that could occur during the blade's service life together with their probability of occurrence. The long-term erosion damage rate is given by

$$\dot{D}_i^{LT} = \sum_i^{\infty}\sum_j^{\infty}\sum_k^{\infty} \dot{D}_i^{ST}(I, \phi_d, U_w) \cdot f_{I,\phi_d}(I_i, \phi_{dj}) \cdot P(I_i) \cdot f_{U_w}(U_{w_k})\ \Delta I\ \Delta\phi_d\ \Delta U_w \tag{18}$$

where $\dot{D}_i^{LT} \geq 1$ implies the end of incubation time. $P(I_i)$ in the above equation describes the percentage of time rain of a given intensity falls at a given site. One of the important checks during the analysis is to make sure that all possible rain and wind condition for a given site are included for the analysis. Thus, it is essential to check that the area under the PDF curve is approximately 1 that is, the equation below is satisfied:

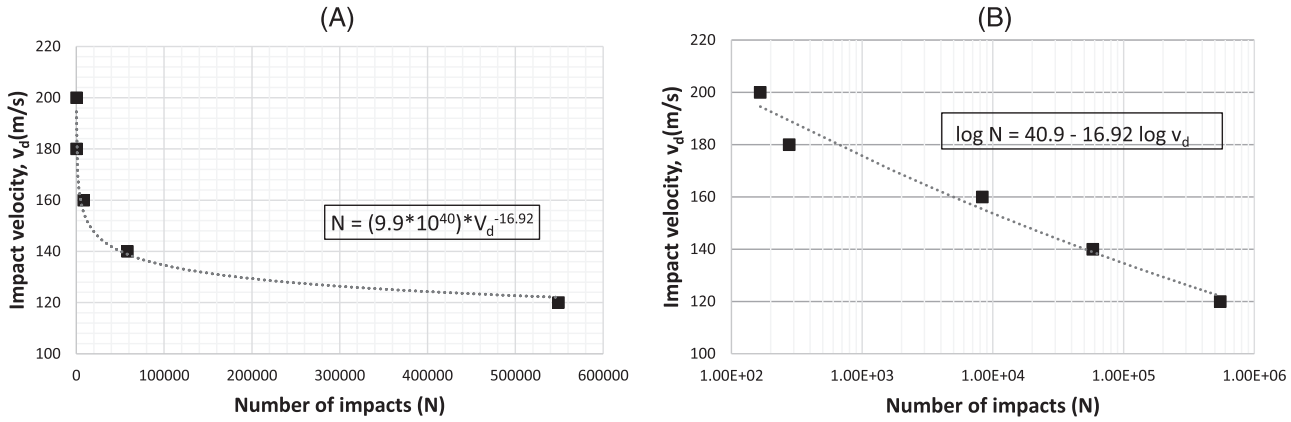

FIGURE 7 'V_d–N' curve shown by (A) power law and (B) with logarithmic x axis (N represents number of impacts at the end of incubation)

TABLE 2 Properties for the PU coating[22,53]

ρ_s	c_s	σ_u	m	ν
1100 kg/m^3[22]	1900 m/s[51]	37 MPa[52]	16.92	0.3[22]

$$\int_i \int_j \int_k f_{I,\phi_d}(I_i,\phi_{dj}) \cdot f_{U_w}(U_{w_k})\, dI \cdot d\phi_d \cdot \cdot dU_w \approx 1 \tag{19}$$

Finally, the expected lifetime for the blade coating system, in years (t_{years}), is defined by

$$t_{years} = \frac{1}{\dot{D}_i^{LT} \cdot (365 \cdot 24)} \tag{20}$$

where $\dot{D}_i^{LT}$ is defined in h^{-1}. The number of repairs (N) expected to occur during the blade service life is then given by

$$N = \frac{t_{total}}{t_{years} \cdot \eta}; \quad 1 \le \eta \le 3 \tag{21}$$

where t_{total} is the total blade service life (in years) and is considered as 25 years in this paper and η is considered as the fraction of waiting time post the incubation period before the repair activities are conducted for WTBs. According to Springer and Baxil,[26] η can vary between 1 and 3, where 1 represents end of incubation time and 3 represents complete failure of the coating material. In this study, η is assumed as 1.5 (Figure 8). This means that a repair waiting time equal to half of the coating lifetime is considered. This value is chosen based on industrial discussions given that the repair activities are not generally performed exactly after the first surface damage on the blade surface is observed. Note that this factor is industry specific and the urgency to repair depends upon varying O&M strategies and different damage types[54] such as if damage penetrates down to the leading-edge protection or through the entire laminate thickness.

3.6 | Details of case studies

Case studies are performed for two turbines with distinct power ratings—NREL WindPact 1.5 MW[55] and DTU 10 MW wind turbine.[56,57] The power curve and the corresponding specifications that are important for modelling of wind turbine are shown in Figures 9A,B. Note that it is assumed in this study that both the turbines are commercially feasible to be installed at all the 31 sites for sake of comparison. However, in practice, feasibility studies are performed before making such a choice for installing a wind turbine.

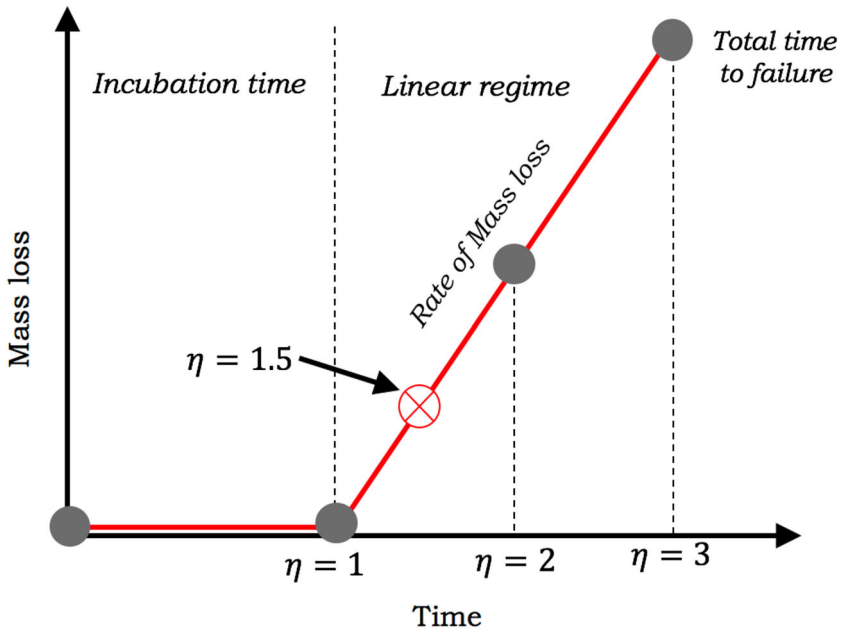

FIGURE 8 Leading-edge lifetime (LEL) as described by the Springer's erosion model

4 | RESULTS AND DISCUSSION

4.1 | Rain characteristics for different sites

Figure 10A presents the comparison of rain intensity data for station number 277 (Lauwersoog) plotted on gamma and lognormal quantile–quantile (Q–Q) plots. A quantile–quantile (Q–Q) plot is referred to as a statistical method where two probability distributions are compared by graphing their quantiles or percentiles against each other. If the data on the graph shows approximately a straight line, then the data is considered

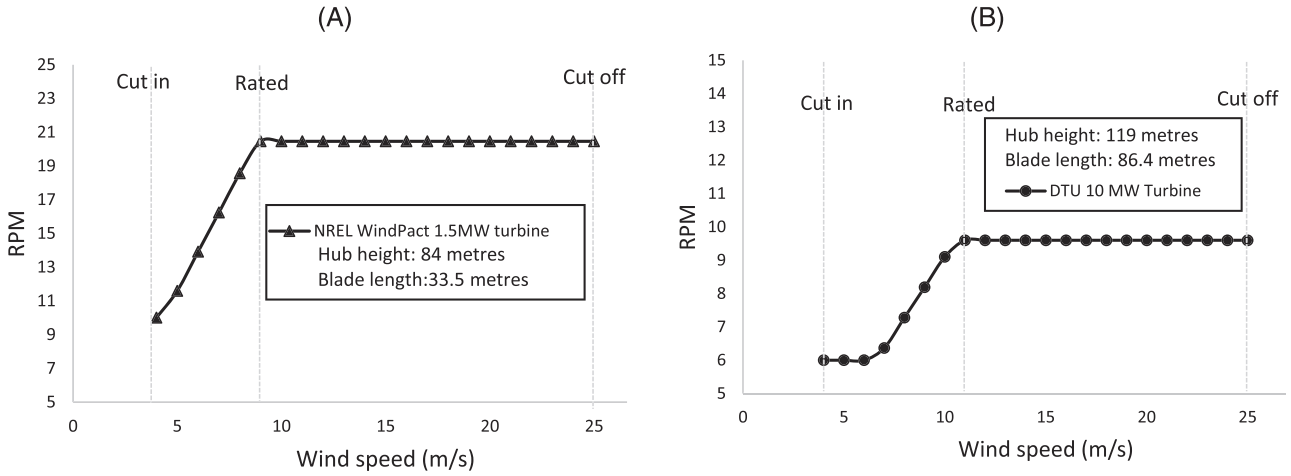

FIGURE 9 (A) Power curve for NREL WindPact 1.5 MW wind turbine. (B) Power curve for DTU 10 MW wind turbine

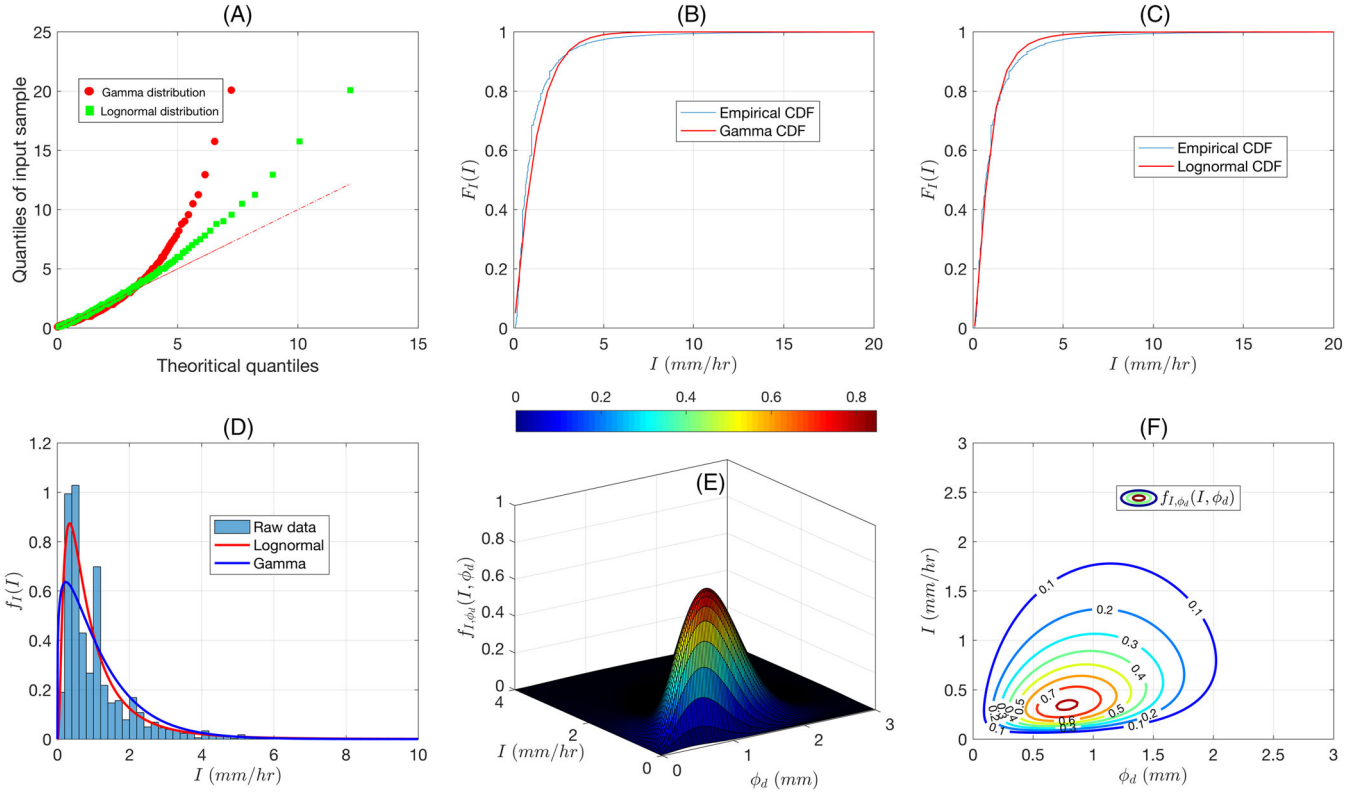

FIGURE 10 Probabilistic rainfall model results for Site 277 (Lauwersoog). (A) Comparison of Q–Q plot for rain intensity data; comparison of empirical CDF with (B) gamma CDF and (C) lognormal CDF. (D) Comparison of raw data with lognormal and gamma distributions; joint PDF of I and ϕ_d. (E) 3D surface plot. (F) 2D contour plot

to be well represented by the considered distribution. It is found from the analysis that for the given site, data for rain intensities is better represented by lognormal distribution compared to gamma distribution. This is also confirmed from goodness of fit test performed using χ^2 method, where the lognormal distribution defined through the null hypothesis is found to be not rejected at 5% significance level. A comparison between empirical and theoretical cumulative distribution function (CDF) for the rain intensity data using both the distributions (Figures 10B,C) also shows large difference for the case of gamma distribution compared to lognormal distribution. Finally, in Figure 10D, a histogram representing the raw rain data is plotted against the distribution of lognormal and gamma, and it can be confirmed that lognormal distribution is an appropriate distribution fit for the rain intensity. Note that Figure 10D clearly shows that the nature of distribution of rain intensity is skewed to the right and that most of the rainfall is associated with light rainfall conditions (I < 2.5 mm/h) for the given site. Further, this distribution is then combined with Best's DSD and the joint probabilistic distributions of droplet size (ϕ_d) and rainfall intensity (I) is obtained for this site. The joint PDF is shown by a three dimensional (3D) surface plot in Figure 10E and two-dimensional (2d) contour plot in Figure 10F. It can be observed from these figures that there is a large probability of occurrence for rain conditions associated with low intensity rainfall conditions (I < 2.5 mm/h) along with droplet size varying in the range of 0.2 to 2 mm. One of the advantages of the joint PDF is that it describes the probability of simultaneous occurrence of rain intensity and associated droplet size during precipitation. For instance, it can be obtained that the probability of simultaneous occurrence of rain intensity 0.5 mm/h and droplet size 1 mm is approximately 0.697 (69.7%) for the considered site.

A similar approach is used for all the remaining 30 sites considered in this paper. For instance, Figures 11A,C present the results for the probabilistic rain model for station number 348 (Cabauw), where it can again be seen that the lognormal distribution presents a good distribution fit for the rain intensity compared to gamma distribution. Further, like the previous station, most of the rainfall at this site is also associated with light rainfall conditions (I < 2.5 mm/h) which are shown in Figure 11D. Note that compared to the site 277, there is a difference in the magnitude of joint distribution function of intensity and rain droplet size which can be seen by comparing Figures 10E,F and 11E,F. For instance, the probability of simultaneous occurrence of rain intensity 0.5 mm/h and droplet size 1 mm is around 0.622 (62.2%) for site 348 compared to 69.7% for the site 277. Finally, for all the sites, the distribution parameters (μ and σ) for describing the rain intensity through the lognormal distribution is obtained and tabulated in Table 3.

A geographic bubble chart representing the spatial variation in the median rainfall intensity for all the sites is presented in Figure 12. Note that the median, compared to the mean, is a more appropriate statistical parameter to represent the measure of central tendency for the rain intensity data. This is because the distribution of rain intensity is skewed to the right and not symmetrical. In the figure, the size and colour of the

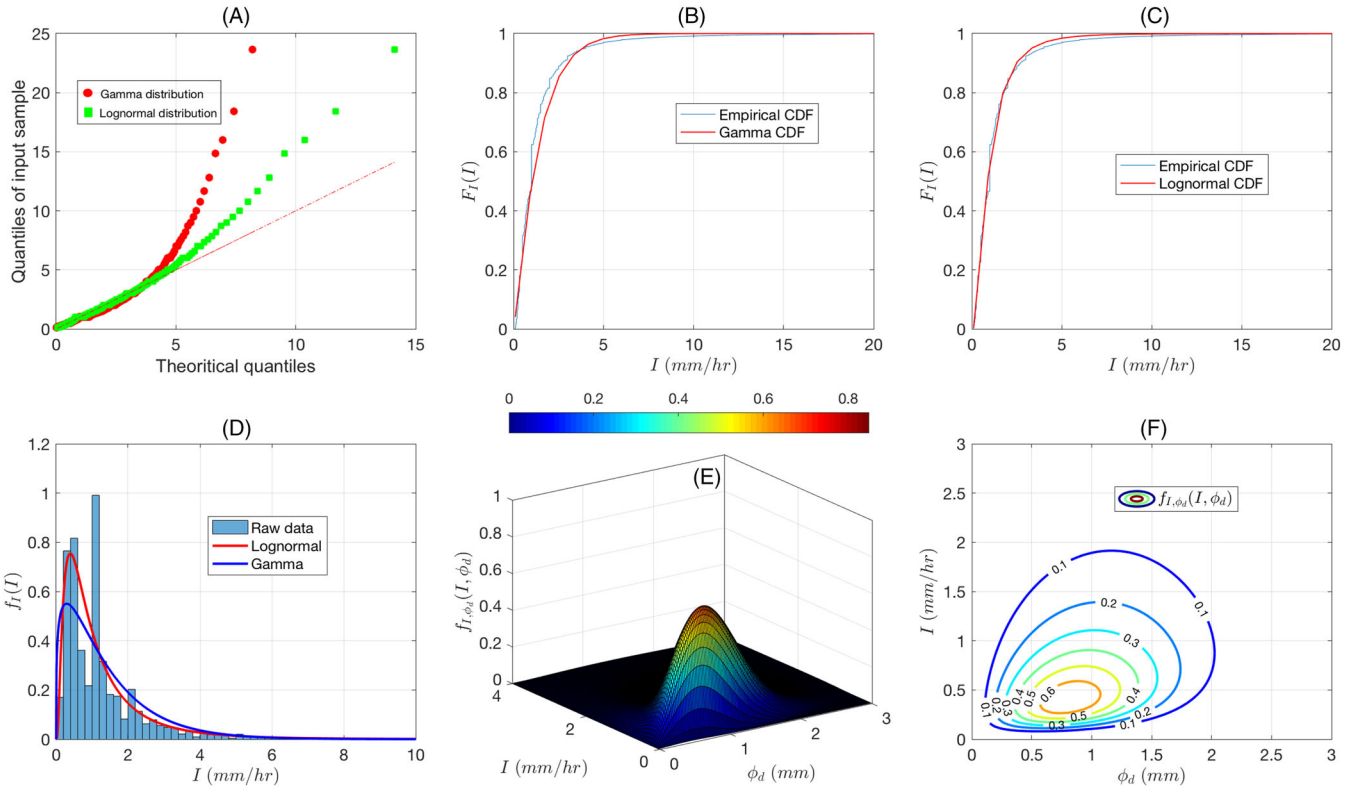

FIGURE 11 Probabilistic rainfall model results for Site 348 (Cabauw). (A) Comparison of Q–Q plot for rain intensity data; comparison of empirical CDF with (B) gamma CDF and (C) lognormal CDF. (D) Comparison of raw data with lognormal and gamma distributions; joint PDF of I and ϕ_d. (E) 3D surface plot. (F) 2D contour plot

TABLE 3 Summary of different statistical parameters calculated for all the Dutch sites

Station no.	Site name	α_u	β_u	μ	σ	P_1(%)	P_2(%)	P_3(%)	P_4(%)
210	Valkenburg	1.831	7.984	−0.162	0.863	10.339	1.420	0.1004	0.0009
235	De kooy	1.963	9.082	−0.233	0.880	10.287	1.300	0.0845	0.0008
240	Schiphol	1.894	8.084	−0.208	0.897	10.490	1.402	0.0939	0.0012
249	Berkhout	1.909	7.891	−0.200	0.828	10.918	1.360	0.0834	0.0016
251	Hoorn (terschelling)	2.117	10.156	−0.205	0.826	10.826	1.352	0.0891	0.0013
260	De bilt	1.963	5.583	−0.247	0.872	10.601	1.271	0.0900	0.0012
267	Stavoren	2.078	9.452	−0.250	0.831	10.360	1.204	0.0686	0.0021
269	Lelystad	1.917	7.069	−0.243	0.885	10.401	1.215	0.1052	0.0004
270	Leeuwarden	1.928	7.512	−0.226	0.840	11.011	1.309	0.0888	0.0008
273	Marknesse	1.932	6.836	−0.268	0.850	10.696	1.178	0.1016	0.0021
275	Deelen	1.880	6.261	−0.276	0.888	10.887	1.241	0.0958	0.0016
277	Lauwersoog	2.145	10.187	−0.274	0.806	11.378	1.225	0.0707	0.0004
278	Heino	1.824	5.260	−0.320	0.848	10.361	1.066	0.0944	0.0004
279	Hoogeveen	1.918	6.471	−0.271	0.855	10.892	1.224	0.0921	0.0021
280	Eelde	1.882	6.850	−0.285	0.881	11.132	1.240	0.0896	0.0012
283	Hupsel	1.872	5.545	−0.325	0.858	10.269	1.038	0.0936	0.0021
286	Nieuw beerta	2.024	7.994	−0.337	0.819	11.004	1.050	0.0802	0.0008
290	Twenthe	1.901	5.747	−0.325	0.914	10.327	1.083	0.0993	0.0004
310	Vlissingen	1.990	9.848	−0.229	0.900	9.579	1.199	0.0997	0.0008
319	Westdorpe	1.813	6.794	−0.245	0.871	9.812	1.146	0.0885	0.0017
323	Wilhelminadorp	1.939	7.654	−0.235	0.834	10.166	1.228	0.0809	0.0010
330	Hoek van holland	2.244	11.427	−0.192	0.833	10.218	1.314	0.0914	0.0014
344	Rotterdam	1.815	7.184	−0.195	0.884	10.417	1.396	0.0958	0.0004
348	Cabauw	1.843	6.911	−0.128	0.807	9.823	1.248	0.0939	0.0012
350	Gilze-rijen	1.963	5.958	−0.301	0.921	10.111	1.132	0.0993	0.0004
356	Herwijnen	1.814	6.576	−0.266	0.839	10.186	1.099	0.0932	0.0013
370	Eindhoven	1.882	6.142	−0.324	0.928	9.713	1.058	0.0970	0.0016
375	Volkel	1.794	5.980	−0.298	0.897	9.542	1.068	0.0923	0.0027
377	Ell	1.795	5.806	−0.309	0.882	9.318	0.995	0.0879	0.0011
380	Maastricht	1.900	6.746	−0.347	0.919	9.903	1.025	0.0942	0.0012
391	Arcen	1.848	5.150	−0.322	0.868	9.488	0.987	0.0865	0.0008

Note: α_u and β_u are shape and scale parameters for the Weibull distribution representing wind speed data at hub height of 119 m; μ and σ are lognormal distribution parameters representing the rain intensity data; P_1, P_2, P_3, and P_4 describe the percentage of rain associated with light, moderate, heavy, and very heavy rainfall condition, respectively.

bubbles represents the magnitude and severity of the data. A high severity (shown by the red bubbles) represents median rainfall intensity between 0.8 mm/h and 1 mm/h, medium severity (shown by the orange bubbles) implies median rainfall intensity between 0.75 and 0.8 mm/h, and low severity (shown by the yellow bubbles) implies median rainfall intensity between 0.6 and 0.75 mm/h. It can be seen from the figure that the median rain intensity for all the sites ranges between 0.67 to 1 mm/h and is highest for the coastal sites compared to the inland sites. This observation is in line with previous meteorological reports where it has been observed that the prevailing westerly winds in the Netherlands bring moisture from the ocean to the land, and therefore coastal areas have higher amounts of precipitation than inland areas. This influence is more dominant in the first 50 km from the coast, as can be observed from the bubble chart and also reported in Manola et al.[58] Note that there are other factors as well that affects the precipitation amount for a given site such as the urbanisation, city size, wind direction, etc. The reader is suggested to refer to Manola et al.[58] for more information on spatial variability of rainfall in the Netherlands. It is to be noted that the above analysis for determining the best distribution fit for the rain data and the associated joint PDF represent the *'wet periods'* for a given site which accounts for only the rain hours. However, rainfall is not a continuous phenomenon and there are periods of time when there is no rain intensity calculated, which is taken as the *'dry periods'* for a given site in this study. This aspect is quantified in the proposed long-term framework by a

correction factor $P(I)$ which determines the percentage of time a rain of a given intensity falls at a given site. This parameter can further be categorised as 'P_1' that describes the percentage of rain associated with light rainfall conditions ($0.0 < I < 2.5$ mm/h), 'P_2' that describes the percentage of rain associated with moderate rainfall conditions ($2.5 \leq I < 10$ mm/h), and 'P_3' and 'P_4' that describe the percentage of rain associated with heavy ($10 \leq I < 50$ mm/h) and very heavy rainfall condition ($I \geq 50$ mm/h), respectively. These parameters are tabulated in Table 3 and it can be seen that the light rainfall conditions (P_1) dominate for all the sites and range between 9% to 12% all over the Netherlands followed by moderate rainfall conditions (P_2). Also, for all the sites, P_3 and P_4 that represents heavy and very heavy rainfall are found to be almost negligible.

4.2 | Wind characteristics for different sites

The discussion regarding wind statistics model is made with respect to DTU 10 MW turbine that is associated with 119 m hub height. Figure 13A–C compare the mean wind speeds plotted on respective Weibull and lognormal quantile–quantile plot for three different sites. These

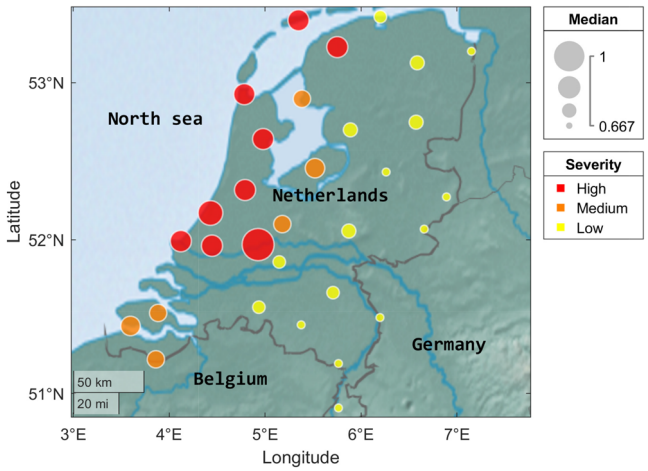

FIGURE 12 Geographic bubble chart representing median rainfall intensity (in mm/h)

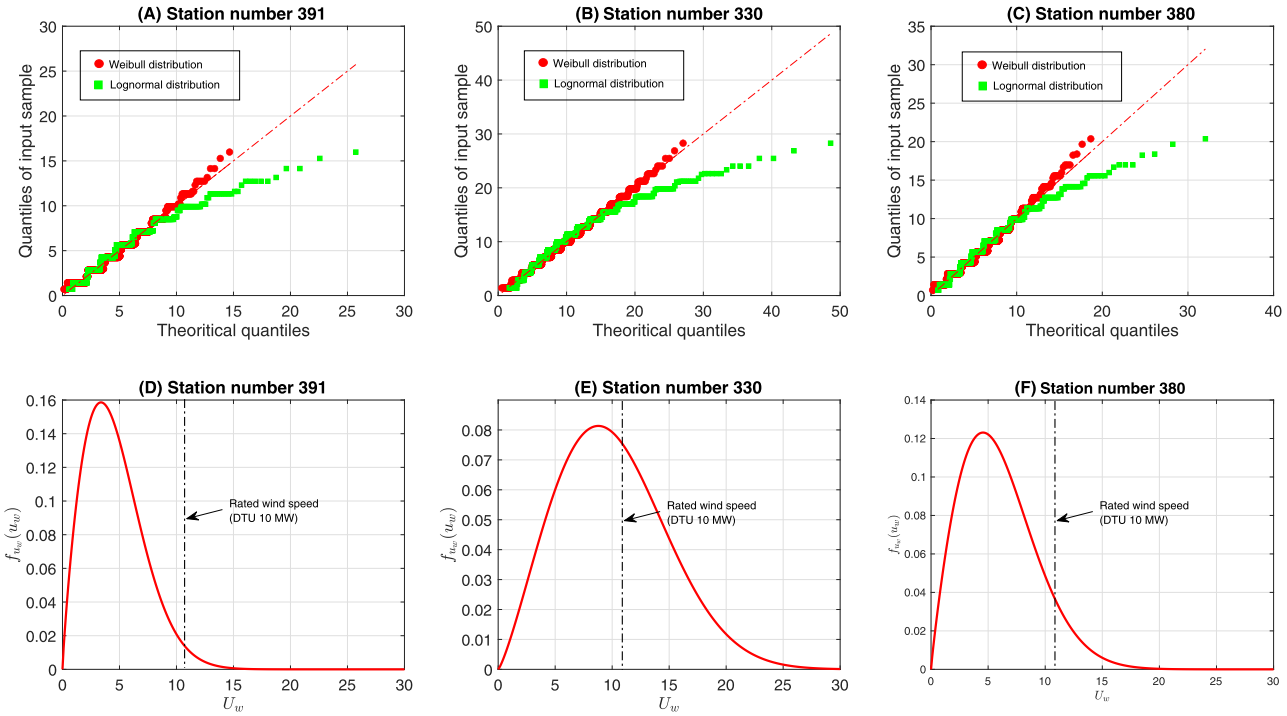

FIGURE 13 Wind statistics results—Comparison of Weibull and lognormal Q–Q plot for (A) station no. 391 (Arcen), (B) station no. 330 (Hoek van Holland), and (C) station no. 380 (Maastricht).Comparison of wind speed PDF at the hub height (119 m) for (D) station no. 391 (Arcen), (E) station no. 330 (Hoek van Holland), and (F) station no. 380 (Maastricht)

sites represent distinct spatial features—station no. 391 (Arcen) is an inland site, station no. 330 (Hoek van Holland) is a coastal site and finally station no. 380 (Maastricht) is an inland site having an altitude of 114 m. It is obvious from these figures that the Weibull distribution gives the best distribution fit for representing mean wind speed for all these sites. Also, the respective shape (α_u) and scale (β_u) parameters for all the sites are obtained and listed in Table 3. Based on these distribution parameters the PDFs of the mean wind speed can be obtained and are shown in Figure 13D–F for the above mentioned sites. As expected, there are higher ranges of wind speeds for the coastal site compared to the other two inland sites.

It is interesting to observe that the area under the PDF curve post the rated wind speed of DTU 10 MW turbine (i.e., 11.4 m/s) is the highest for the coastal site followed by station no. 380 (Maastricht) which has an altitude of 114 m and the inland station no. 391 which has an altitude of 20 m. Note that this observation is expected to have noticeable implications on the calculations of the expected lifetime of the coating system for a given site, as the blade is expected to rotate at its highest tip speed above the rated wind conditions. A comparison between the exceedance probability for rated wind conditions for six different sites with varying spatial features is shown in Figure 14A. The coastal sites are found to have higher probability of exceedance for the rated wind speed, and thus it is expected to have blade rotating at the largest tip speed (e.g., 90 m/s for DTU 10 MW blade) for large periods of time compared to other inland sites. It is also essential to compare the Weibull scale parameters for different wind turbine sites as this parameter indicates where the peak of the wind distribution lies. A geographic bubble chart representing the spatial variation of the scale parameter of the mean wind speed for the considered sites is presented in Figure 14B. In the figure, the size and colour of the bubbles represents the magnitude and severity of the data. A high severity (shown by the red bubbles) represents scale parameters between 9 and 12 m/s, medium severity (shown by the orange bubbles) implies scale parameters between 7 and 9 m/s, and low severity (shown by the yellow bubbles) implies scale parameters between 5 and 7 m/s. It can be seen that the scale parameter ranges approximately between 5 and 11.5 m/s, is the largest for the coastal sites, and reduces towards the inland sites; that is, the majority of the bubbles along the coastal areas represent high severity and larger bubble size. Also, Maastricht (station no. 380) which has the highest altitude is associated with a relative larger bubble size compared to surrounding low lying inland locations, and thus the data plotted on geographical bubble chart captures the orographic effects.

4.3 | Expected leading-edge lifetime and number of repairs

Figures 15A,B present the geographic bubble chart displaying the spatial distribution of the expected lifetime of the blade coating system calculated for DTU 10 MW and NREL WindPact 1.5 MW wind turbine, respectively, using the proposed long-term framework. The size and the colour of the bubbles represent the magnitude and severity of the calculated leading-edge lifetime for all the considered sites in the Netherlands. A high erosion severity (shown by the red bubbles) represents coating lifetime less than 2 years, medium severity (shown by the orange bubbles) implies coating lifetime between 2 and 4 years, and low severity (shown by the yellow bubbles) represent coating lifetime above 4 years. It can be seen from the first figure that the expected lifetime for the 10 MW wind turbine varies between 0.867 and 7.184 years, with higher erosion obtained for the coastal sites compared to the inland sites. This is in line with the results presented in the previous discussions where coastal sites were found to have larger probability of exceedance of rated wind conditions together with higher median rainfall intensity and greater precipitation duration. As a result, turbines at coastal locations are expected to rotate at their largest tip speed for most of the time as compared to the inland sites, and this leads to higher erosion while being exposed to rainfall. The lowest expected lifetimes for blade coating system are found at the

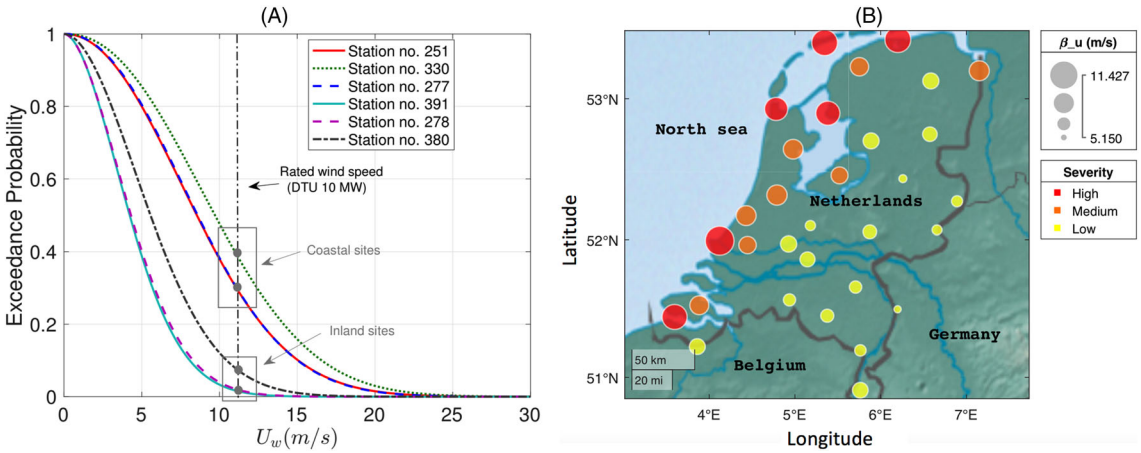

FIGURE 14 (A) Exceedance probability of rated wind speed for coastal and inland sites. (B) Geographic bubble chart representing Weibull scale parameters

coastal sites—Hoek van Holland (station no 330), Hoorn (Terschelling) (station no 251) and Lauwersoog (station no 277)—compared to the inland De Bilt site where expected lifetime is found to be approximately 5 years (see white arrows in Figure 15A where these sites are marked with 'HvH', 'H', 'L', and 'De', respectively). Further, the average expected lifetime of leading-edge coating system is also calculated for all the inland and coastal sites considered in this study along with standard error and shown in Figure 16. The average expected lifetime for a WTB is found to be approximately 3 times lesser for turbines operating at coastal sites compared to the inland sites and this observation is in line with findings made in other proposed frameworks.[12,14] It is also interesting to note that Maastricht (station no. 380) and Deelen (station no. 275) that have high altitudes are found to have relatively faster erosion compared to the surrounding inland locations (see white arrows in Figure 15A) where these sites are marked with 'M' and 'D', respectively). This is primarily due to the fact that the site is associated with higher wind speeds and larger exceedance probability for rated wind conditions compared to surrounding inland sites. Overall, the erosion bubble chart calculated through the proposed long-term framework captures the effects of spatial and orographic features of the sites on LEE calculations. The second figure (Figure 15B) presents the geographical bubble chart for expected lifetime for NREL WindPact 1.5 MW wind turbine. It can be seen that the erosion for this turbine follows the same trend as shown by the DTU 10 MW wind turbine in terms of spatial and orographic effects, that is, faster erosion at coastal sites as well as sites associated with higher altitudes. However, compared to DTU 10 MW turbine, there is at least 2 times increase in the overall expected lifetime of blade coating system. The expected lifetime for the considered turbine is in the range of approximately 2.3 to 14.9 years. A detailed quantitative comparison is presented in Table 4. The increase in the incubation time is attributed to the turbine specifications for the NREL 1.5 MW wind turbine that has a tip speed of 75 m/s, and a hub height of 84 m compared to the DTU 10 MW wind turbine that has a hub height of 119 m, and rated tip speed of 90 m/s. It is to be also noted that the damage erosion rate according to the Springer's erosion model is almost proportional to the 6.7th power of the impact velocity. Hence, reduction in the tip speed of the blade from 90 to 75 m/s and

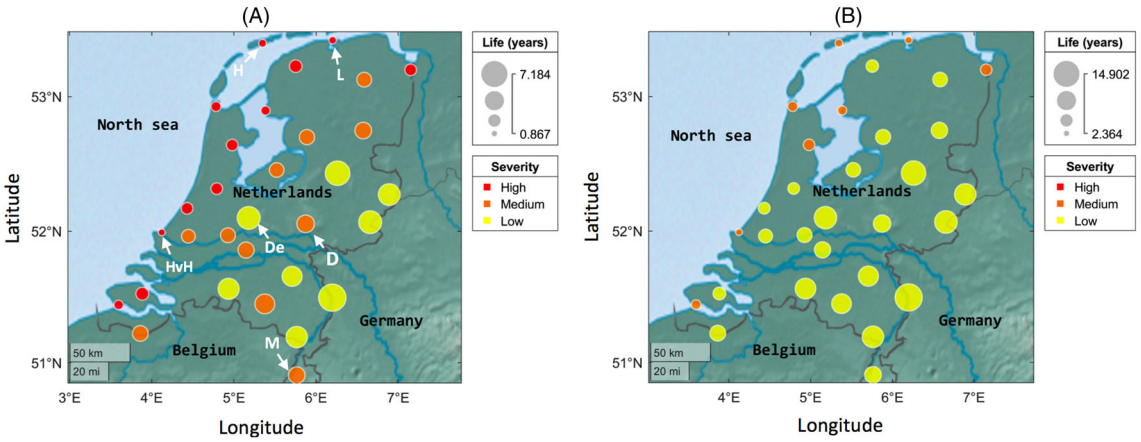

FIGURE 15 Geographic bubble chart representing expected lifetime for WTB coating system (A) DTU 10 MW and (B) NREL 1.5 MW wind turbine

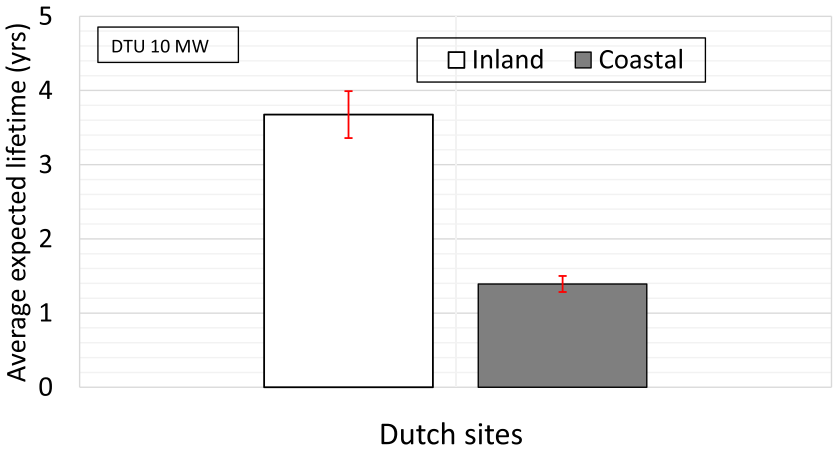

FIGURE 16 Comparison of average erosion lifetime for WTB at inland and coastal sites

TABLE 4 Summary of lifetime and number of repairs calculated for different sites and turbines

KNMI station number	KNMI site name	DTU 10 MW wind turbine		NREL 1.5 MW wind turbine	
		Lifetime (years)	No. of repairs	Lifetime (years)	No. of repairs
210	Valkenburg	1.664	10	4.057	4
235	De kooy	1.323	12	3.348	4
240	Schiphol	1.651	10	4.003	4
249	Berkhout	1.636	10	3.910	4
251	Hoorn (Terschelling)	0.994	16	2.601	6
260	De bilt	5.187	3	10.600	1
267	Stavoren	1.200	13	3.050	5
269	Lelystad	2.374	7	5.364	3
270	Leeuwarden	1.866	8	4.333	3
273	Marknesse	2.541	6	5.626	2
275	Dee len	3.242	5	6.993	2
277	Lauwersoog	0.948	17	2.478	6
278	Heino	5.899	2	12.300	1
279	Hoogeveen	2.941	5	6.369	2
280	Eelde	2.412	6	5.412	3
283	Hupsel	5.169	3	10.753	1
286	Nieuw beerta	1.662	10	3.911	4
290	Twenthe	4.742	3	9.879	1
310	Vlissingen	1.235	13	3.225	5
319	Westdorpe	2.676	6	6.087	2
323	Wilhelminadorp	1.929	8	4.513	3
330	Hoek van holland	0.867	19	2.364	7
344	Rotterdam	2.156	7	5.026	3
348	Cabauw	2.459	6	5.594	2
350	Gilze-rijen	4.446	3	9.221	1
356	Herwijnen	2.810	5	6.299	2
370	Eindhoven	3.985	4	8.527	1
375	Volkel	4.083	4	8.856	1
377	Ell	4.590	3	9.852	1
380	Maastricht	2.950	5	6.544	2
391	Arcen	7.184	2	14.902	1

the associated reduced hub height extends the overall incubation time of the blade coating system. All in all, the proposed framework efficiently captures the effects of spatial and orographic features of the sites and wind turbine specifications on LEE calculations.

Figure 17A,B presents the geographical bubble chart displaying the spatial distribution of expected number of repairs required for DTU 10 MW and NREL WindPact 1.5 MW wind turbine, respectively, during the turbines' service life. The size and the colour of the bubbles represent the magnitude and severity associated with the number of repairs required for the turbine blades. A high severity represents the sites that require more than 12 number of repairs over their service life, medium severity represents the sites that require 5 to 12, and low severity represent number of repairs less than 5. As expected and in line with the previous discussions, the number of repairs is highest near the coastal sites and low for the inland sites and ranges from 2 to 19 for the considered DTU 10 MW blade. A similar trend is seen in the second figure for the NREL 1.5 MW wind turbine where it is still expected to have more number of repairs at the coastal sites, however, the number of repairs ranges from 1 to 7. A detailed quantitative comparison is presented in Table 4. Notice that the erosion bubble chart for the total number of repairs also captures the orographic aspect where sites Masstrict and Deelen are found to have a moderate severity (shown in orange bubble in Figure 17A) compared to other surrounding inland sites which are associated with low severity (shown in yellow bubble). Overall, from the above discussions, it can be clearly observed that the LEE is a site-specific problem and is sensitive to the chosen turbine type. Although increasing the turbine size is expected to increase the power output, it also increases the probability of faster erosion, thus leading to large repair costs. The proposed method

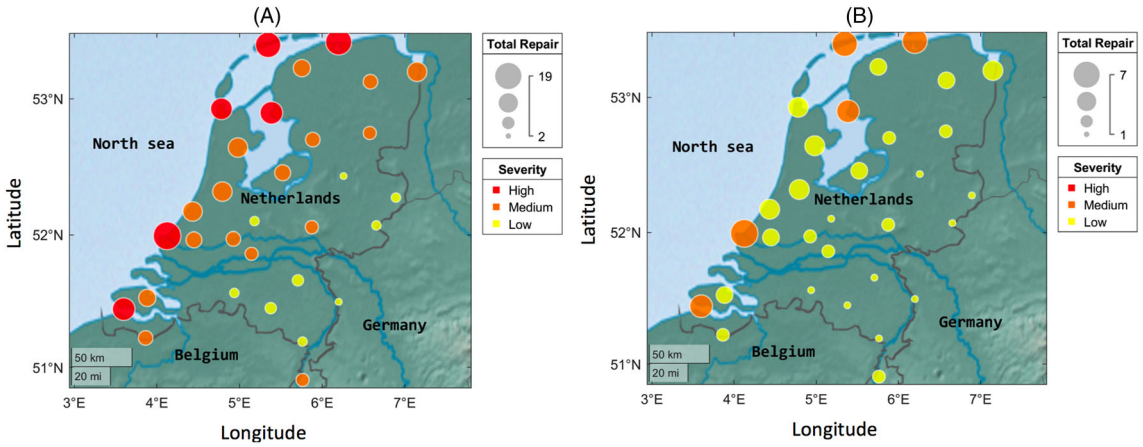

FIGURE 17 Geographic bubble chart for expected number of repairs required over the blade service life (A) DTU 10 MW and (B) NREL 1.5 MW wind turbine

in this paper can thus be used to perform LEE analysis by considering site-specific environmental parameters along with choice of a suitable coating system and estimate site-specific repair cost. In this way, the proposed framework can be used during the pre-design phase to perform an efficient trade-off analysis for all the important aspects related to the economics of erosion: choice of site, turbine type, best coating solution and associated repair and maintenance costs.

5 | CONCLUSIONS

The current paper proposed a probabilistic long-term framework for assessing site-specific lifetime of a WTB coating system. Case studies were presented for 1.5 and 10 MW turbines where geographic bubble charts for the leading-edge lifetime and number of repairs expected during the blade's service life are established for 31 sites in the Netherlands. Following are the main conclusions that were obtained from this study:

1. It was found from the probabilistic rainfall model that the coastal sites have a relatively high median rainfall intensity and are associated with a larger duration of precipitation hours compared to the inland sites.
2. It was also found in the study that coastal sites have higher exceedance probability of rated wind speed. This implies turbines rotating at maximum tip speed, thereby developing higher rain-induced erosion than the inland sites.
3. From the analysis, it was clearly observed that the coastal sites have 3 times reduced leading-edge lifetime and will require a higher number of repairs compared to the inland sites, and this effect increased with increasing power rating together with higher tip speed.
4. Overall, the proposed framework is found to efficiently capture the effects of spatial and orographic features of the sites and wind turbine specifications on LEE calculations.

6 | LIMITATIONS AND RECOMMENDATIONS FOR FUTURE WORK

A list of assumptions, limitations and recommendations for future work are presented below. Note that the recommendations made below are listed in the order of importance for improving the proposed framework.

1. In this study, different sites were considered for verifying the numerical model for calculating the growth of erosion of wind turbines. However, it is important to have a real scale validation of the modelling approach proposed in the paper.
2. In the current study, only the effects of mean wind speed at the hub height were considered for calculating the impact velocity. However, the study in Verma et al.[59] shows that the turbulence intensity (TI) also has a considerable effect on the impact velocity and the erosion damage rate. In the future, efforts will be made to include the effects of TI in the proposed framework. Also, the statistical dependence between rain and wind will be considered.
3. Only simplified WT models consisting of RPM schedule are used to derive the blade tip speed. Several factors are ignored, for example, control strategy of a WT, effects of varying rotor azimuth angle, effects of droplet impact angle, aeroelasticity, as well as the disturbance caused in the

trajectory of the rain droplet due to aerodynamic effects while the blade is rotating. In the future, more work will be performed to improve these aspects.

4. In this study, Springer's surface fatigue model for homogeneous material[26] was considered for evaluating short-term erosion damage rate. In the future, erosion models that include the effects of droplet, coating and substrate interactions during droplet impingement will be considered.
5. In the current paper, the site-specific variation in the LEE calculations were considered only by varying rain and wind conditions for different sites. However, other environmental parameters such as the temperature and humidity of the site, as well as the salinity of the rainwater are also expected to cause such variations. More work is required in the future to understand these effects and include them in the model.

7 | SUGGESTIONS AND RECOMMENDATIONS FOR WT DESIGNERS/OWNERS

In addition to the discussions above, following are some suggestions and recommendations to the WT designers/owners:

1. The erosion modelling framework proposed in the study can be used to calculate site-specific lifetime of WTB coating system at real scale. However, it is essential to have a reliable dataset for precipitation statistics, especially the distribution of droplet size which is site-specific. It is recommended to instal measurement devices at the turbine site to record the essential droplet statistics with high accuracy.
2. WT designers or operators can use this framework as a tool during the pre-design phase to perform an efficient trade-off analysis for all the important aspects related to the economics of erosion: choice of site, turbine type, best coating solution and associated repair and maintenance costs. The proposed framework also aids in comparing different coating performance as well as associated repair costs at real scale.
3. The material characteristics such as the Wöhler slope is an essential parameter for the LEE analysis. These data are rarely available in a typical coating datasheet and requires time consuming and costly water erosion tests. The authors encourage coating suppliers to provide these inputs in the datasheet that would aid in obtaining reliable estimates of coating lifetime using the proposed framework.

ACKNOWLEDGEMENT

This work was made possible through the Rijksdienst voor Ondernemend Nederland (RVO) funded WINDCORE project having subsidy scheme TSE–18–04–01–Renewable energy project with project number TEHE118013. The authors highly appreciate the financial support.

PEER REVIEW

The peer review history for this article is available at https://publons.com/publon/10.1002/we.2634.

DATA AVAILABILITY STATEMENT

The data that support the findings of this study are available from the corresponding author upon reasonable request.

ORCID

Amrit Shankar Verma https://orcid.org/0000-0002-1021-0613
Zhiyu Jiang https://orcid.org/0000-0002-8778-0999

REFERENCES

1. Verma AS, Jiang Z, Vedvik NP, Gao Z, Ren Z. Impact assessment of a wind turbine blade root during an offshore mating process. *Eng Struct*. 2019;180:205-222.
2. IRENA. Future of wind deployment, investment, technology, grid integration and socio-economic aspects. Accessed: 2020-08-11; 2019.
3. Pugh K, Rasool G, Stack MM. Raindrop erosion of composite materials: some views on the effect of bending stress on erosion mechanisms. *J Bio-and Tribo-Corrosion*. 2019;5(2):45.
4. Doagou-Rad S, Mishnaevsky Jr L, Bech JI. Leading edge erosion of wind turbine blades: Multiaxial critical plane fatigue model of coating degradation under random liquid impacts. *Wind Energy*. 2020;23(8):1752-1766.
5. Burton T, Sharpe D, Jenkins N, Bossanyi E. *Wind Energy Handbook*. New York: John Wiley & Sons; 2011.
6. Keegan MH, Nash D, Stack M. Modelling rain drop impact on offshore wind turbine blades. *ASME Turbo Expo 2012*. 2012:Article-GT.
7. Keegan MH, Nash DH, Stack MM. On erosion issues associated with the leading edge of wind turbine blades. *J Phys D: Appl Phys*. 2013;46(38):383001.
8. Verma AS, Castro SaulloGP, Jiang Z, Teuwen JulieJE. Numerical investigation of rain droplet impact on offshore wind turbine blades under different rainfall conditions: A parametric study. *Composite Struct*. 2020;241:112096.
9. Han W, Kim J, Kim B. Effects of contamination and erosion at the leading edge of blade tip airfoils on the annual energy production of wind turbines. *Renew energy*. 2018;115:817-823.
10. Mishnaevsky Jr L. Repair of wind turbine blades: review of methods and related computational mechanics problems. *Renew Energy*. 2019;140:828-839.

11. Mishnaevsky Jr L. Toolbox for optimizing anti-erosion protective coatings of wind turbine blades: overview of mechanisms and technical solutions. *Wind Energy*. 2019;22(11):1636-1653.
12. Hasager C, Vejen F, Bech JI, Skrzypiński WR, Tilg A-M, Nielsen M. Assessment of the rain and wind climate with focus on wind turbine blade leading edge erosion rate and expected lifetime in Danish seas. *Renew Energy*. 2020;149:91-102.
13. Herring R, Dyer K, Martin F, Ward C. The increasing importance of leading edge erosion and a review of existing protection solutions. *Renew Sustain Energy Rev*. 2019;115:109382.
14. Verma AS, Jiang Z, Marco C, et al. A probabilistic rainfall model to estimate the leading-edge lifetime of wind turbine blade coating system. *Renew Energy*. 2021. (Under review).
15. Brigandì G, Aronica GT. Generation of sub-hourly rainfall events through a point stochastic rainfall model. *Geosciences*. 2019;9(5):226.
16. Tsakiris G. Stochastic modelling of rainfall occurrences in continuous time. *Hydrological Sci J*. 1988;33(5):437-447.
17. https://gcaptain.com/. Picture taken.
18. Picture taken. https://www.armouredge.com/
19. Eisenberg D, Laustsen S, Stege J. Wind turbine blade coating leading edge rain erosion model: development and validation. *Wind Energy*. 2018;21(10):942-951.
20. Mishnaevsky Jr L, Fæster S, Mikkelsen LP, Kusano Y, Bech JI. Micromechanisms of leading edge erosion of wind turbine blades: X-ray tomography analysis and computational studies. *Wind Energy*. 2020;23(3):547-562.
21. O'Carroll A, Hardiman M, Tobin EF, Young TM. Correlation of the rain erosion performance of polymers to mechanical and surface properties measured using nanoindentation. *Wear*. 2018;412:38-48.
22. Keegan MH, Nash D, Stack M. Wind turbine blade leading edge erosion: an investigation of rain droplet and hailstone impact induced damage mechanisms. *PhD thesis*: University of Strathclyde; 2014.
23. Chen J, Wang J, Ni A. A review on rain erosion protection of wind turbine blades. *J Coatings Technol Res*. 2019;16(1):15-24.
24. Amirzadeh B, Louhghalam A, Raessi M, Tootkaboni M. A computational framework for the analysis of rain-induced erosion in wind turbine blades, part I: stochastic rain texture model and drop impact simulations. *J Wind Eng Indust Aerodyn*. 2017;163:33-43.
25. Amirzadeh B, Louhghalam A, Raessi M, Tootkaboni M. A computational framework for the analysis of rain-induced erosion in wind turbine blades, part II: drop impact-induced stresses and blade coating fatigue life. *J Wind Eng Indust Aerodyn*. 2017;163:44-54.
26. Springer GS, Baxil CB. A model for rain erosion of homogeneous materials. *Erosion, Wear, and Interfaces with Corrosion*. West Conshohocken, PA: ASTM International; 1974;106–124.
27. Springer GS, Yang C-I, Larsen PS. Analysis of rain erosion of coated materials. *J Composite Mater*. 1974;8(3):229-252.
28. Springer GS, Yang CI. Model for the rain erosion of fiber reinforced composites. *AIAA J*. 1975;13(7):877-883.
29. Springer GS. Erosion by liquid impact; 1976.
30. Bech JI, Hasager CB, Bak C. Extending the life of wind turbine blade leading edges by reducing the tip speed during extreme precipitation events. *Wind Energ Sci Discuss*. 2018;3(2):729-748.
31. Mishnaevsky Jr L, Sütterlin J. Micromechanical model of surface erosion of polyurethane coatings on wind turbine blades. *Polymer Degradation Stabil*. 2019;166:283-289.
32. Slot HM, Gelinck ERM, Rentrop C, Van Der Heide E. Leading edge erosion of coated wind turbine blades: review of coating life models. *Renew Energy*. 2015;80:837-848.
33. Slot HM, IJzerman RM, le Feber M, Nord-Varhaug K, van der Heide E. Rain erosion resistance of injection moulded and compression moulded polybutylene terephthalate PBT. *Wear*. 2018;414:234-242.
34. Best AC. The size distribution of raindrops. *Quarterly J R Meteorol Soc*. 1950;76(327):16-36.
35. Blom-Zandstra M, Paulissen M, Agricola H, Schaap B. How will climate change affect spatial planning in agricultural and natural environments? Examples from three dutch case study regions, Vol. 8; 2009:12018.
36. Shankar Verma A, Jiang Z, Ren Z, Hu W, Teuwen JJE. Effects of onshore and offshore environmental parameters on the leading edge erosion of wind turbine blades: a comparative study. *J Offshore Mech Arctic Eng*. 2021;143(4):1–15, 042001.
37. Kedem B, Pavlopoulos H, Guan X, Short DA. A probability distribution model for rain rate. *J Appl Meteorology*. 1994;33(12):1486-1493.
38. Cho H-K, Bowman KP, North GR. A comparison of gamma and lognormal distributions for characterizing satellite rain rates from the tropical rainfall measuring mission. *J Appl Meteorology*. 2004;43(11):1586-1597.
39. 61400-3 IEC. Wind turbines, part 3: design requirements for offshore wind turbines; 2009.
40. L. L, Z. G, T. M. Joint distribution of environmental condition at five European offshore sites for design of combined wind and wave energy devices. *J Offshore Mech Arctic Eng*. 2015;137(3):31901-(1–16).
41. Horn J-T, Krokstad JR, Amdahl J. Long-term fatigue damage sensitivity to wave directionality in extra-large monopile foundations. *Proc Inst Mech Eng Part M: J Eng Maritime Environ*. 2018;232(1):37-49.
42. Dong W, Moan T, Gao Z. Long-term fatigue analysis of multi-planar tubular joints for jacket-type offshore wind turbine in time domain. *Eng Struct*. 2011;33(6):2002-2014.
43. Verma AS, Gao Z, Jiang Z, Ren Z, Vedvik NP. Structural safety assessment of marine operations from a long-term perspective: A case study of offshore wind turbine blade installation. In: *International Conference on Offshore Mechanics and Arctic Engineering*. Strathclyde, Glasgow, Scotland: American Society of Mechanical Engineers Digital Collection; 2019;58783, V003T02A074.
44. Verma AS, Jiang Z, Ren Z, Gao Z, Vedvik NP. Response-based assessment of operational limits for mating blades on monopile-type offshore wind turbines. *Energies*. 2019;12(10):1867.
45. Verma AS, Vedvik NP, Gao Z. A comprehensive numerical investigation of the impact behaviour of an offshore wind turbine blade due to impact loads during installation. *Ocean Eng*. 2019;172:127-145.
46. Verma AS, Zhao Y, Vedvik NP, Gao Z. Explicit structural response-based methodology for assessment of operational limits for single blade installation for offshore wind turbines. *Proceedings of the Fourth International Conference in Ocean Engineering (ICOE2018)*, Springer, 2019:737-750.
47. Atlas D, Srivastava RC, Sekhon RS. Doppler radar characteristics of precipitation at vertical incidence. *Rev Geophys*. 1973;11(1):1-35.
48. Papadakis M, Wong S-C, Rachman A, Hung KE, Vu GT, Bidwell CS. Large and small droplet impingement data on airfoils and two simulated ice shapes; 2007.

49. Global Applications Team. Erosion due to inseparable love. https://blog.ducom.com/wind-rain. [Online; accessed 11-Aug-2020].
50. DNVGL. Dnvgl standard dnvgl-rp-0171 testing of rotor blade erosion protection systems; 2018.
51. Ltd Class Instrumentation. Class instrumentation ltd ultrasonic sound velocity table. http://www.classltd.com/sound_velocity_table.html [Online; accessed 03-May-2018].
52. 3M. 3m wind blade protection coating w4600 technical data sheet and application guide. https://multimedia.3m.com/mws/media/978868O/3m-wind-blade-coating-w4600-app-guide-and-technical-data.pdf; 2014.
53. Claus CE. Effects of leading edge erosion on wind turbine efficiency and innovative erosion protection solutions. *Wind Power Monthly Blade Inspection Damage and Repair*. 2013.
54. Bladena V. Instruction—wind turbine blade inspection. EUDP Project LEX and EUDP Project RATZ https://www.bladena.com/uploads/8/1/6/3/81635550/instruction_-_blade_inspections.pdf, Roskilde, Bladena; 2016.
55. Dykes KL, Rinker J. WindPACT reference wind turbines, Golden, CO (United States), National Renewable Energy Lab.(NREL); 2018. NREL/TP-5000-67667.
56. Bak C, Zahle F, Bitsche R, et al. Description of the DTU 10MW reference wind turbine. *DTU Wind Energy Report-I-0092*. 2013;5.
57. Verma AS, Vedvik NP, Haselbach PU, Gao Z, Jiang Z. Comparison of numerical modelling techniques for impact investigation on a wind turbine blade. *Composite Struct*. 2019;209:856-878.
58. Manola I, Steeneveld G-J, Uijlenhoet R, Holtslag AAM. Analysis of urban rainfall from hourly to seasonal scales using high-resolution radar observations in the netherlands. *Int J Climatology*. 2020;40(2):822-840.
59. Verma AS, Jiang Z, Ren Z, Teuwen JJE. Leading edge erosion of wind turbine blades: effects of environmental parameters on impact velocities and erosion damage rate. In: *ASME 2020 39th International Conference on Ocean, Offshore and Arctic Engineering*. American Society of Mechanical Engineers Digital Collection; 2020.

How to cite this article: Shankar Verma A, Jiang Z, Ren Z, et al. A probabilistic long-term framework for site-specific erosion analysis of wind turbine blades: A case study of 31 Dutch sites. *Wind Energy*. 2021;1–22. https://doi.org/10.1002/we.2634